Periodicals of Engineering and Natural Sciences ISSN 2303-4521
Vol. 9, No. 1, January 2021, pp.104-126

Review of the estimation methods for external blast loads on structures

Alan Catovic[1], Elvedin Kljuno[2]
[1] University of Sarajevo, Mechanical Engineering Faculty, Defense technologies department,
[2] University of Sarajevo, Mechanical Engineering Faculty, Department for mechanics,

ABSTRACT

A review of external blast loads on structures modeling methods is presented in the paper. Also, numerical simulations of explosions in an urban scenario were done in software Ansys AUTODYN, and compared to experimental data.
Recommendations were given regarding the use of numerical simulations in blast wave parameter calculations for the urban environment, as well as suggestions for further research.

Keywords: explosion, blast overpressure, structures, external load modeling, simulation

Corresponding Author:

Alan Catovic,
University of Sarajevo
Mechanical Engineering Faculty
Defense Technologies Department
E-mail: catovic@mef.unsa.ba

1. Introduction

After the explosion, the detonation products expand very fast, creating a shock wave with discontinuous pressure peak. When structures are impacted by this wave, they are dragged away from the detonation point, and after that pulled back towards this point. Damage on the structure during this short process depends upon large number of influencing factors.
The most important parameters of explosive shockwaves are maximum overpressure value (blast wave force impacting a surface of the structure) and impulse of the blast (area beneath the pressure-time curve of a wave in positive phase) [2,5].

1.1. Effects of blast on the human body

Generally, reflected blast waves, occurring in an urban environment, are usually more dangerous to the human than incident waves in free airburst scenario. Studies show a higher mortality in enclosed spaces than in open ones, with serious injuries, particularly because of shockwaves reflection [3]. Table 1 shows injuries/deaths in open/enclosed areas.

Table 1. Injuries/deaths in open/enclosed areas (Source: [3])

	Open space	**Enclosed space**
Deaths	8 %	49 %
Injuries:		
- Primary Blast Injuries	34 %	77 %
- Burns (total body surface area)	18 %	31 %

Parts of the body sustaining most severe injuries after the blast wave impacts are: brain (extreme acceleration/deceleration), eyes (contusions, lesions), ears (delicate bones injury), limbs (traumatic amputation), lungs (magnified risk in confined areas), gastro-intestinal tract (fast compression/expansion of the gases), kidneys (can be torn from attachment points inside the body), liver (bruises, tears, punctures).

Structural objects can be damaged from both the positive and negative shockwave phases, but the human body is injured mostly during the positive phase [3]. In Table 2 are shown the effects of explosion blast wave overpressure and wind on human body and structures.

Table 2. Effects of explosion blast wave overpressure and wind on human body and structures (Source: [3])

Peak overpressure (kPa)	Maximum wind speed (m/s)	Effects on the human body	Effects on structures
7	17	Light injuries from fragments	Window glass breaks
14	31	Injuries from flying glass and other debris	Moderate damage on objects (windows, doors blown out, significant roof damage)
21	46	Serious injuries, fatalities also possible	Collapse of urban structures collapse
34,5	73	Widespread fatalities	Most structures collapse
69	131	Most people killed	Reinforced concrete structures severely damaged or crushed
138	224	Fatalities close to 100%	Heavily built concrete structures severely damaged or crushed

1.2. Blast effects in an urban area

In 2020, Beirut was a site of massive explosion of ammonium nitrate storage (2750 tonnes, equiv. to 1.12 kT of TNT charge [14]), causing over 200 casualties, more than 6500 injuries, leaving 300 000 people without homes and accounting for more than 15 billion US$ in damage.

To massively damage a structure, maximum overpressure and impulse must be larger than minimum values required, depending on the type of object. For example, a moderately high overpressure and a low impulse are sufficient for glass breakage. Bricks, on the other hand, require relatively high impulse, and small overpressure values. In a trench, cave, tunnel, or urban street, blast wave pressure decrease is slower comparing to the open areas, because reflections of the wave from the walls are present, and the reflection from several walls can lead to a multiplication on another wall [2].

The location of the charge and the building geometry also influences the distribution of shock wave overpressures. Corridors may cause delayed channelling effect increasing the overpressure. Many cities have a complex building distribution, and the presence of large structures usually leads to lower dispersion of the shockwave energy [6].

The response of the structural object (Table 2) on shock wave depends also on its natural vibration frequency, whereby part of the energy is reflected, and part transmitted to object, depending on the object properties [3].

Research of blast effects and building protection techniques started rapidly to increase worldwide, mainly in order to be able to protect important objects [7].

A response of humans to explosive threat might be to seek protection in buildings and cellars, but this can be dangerous. These objects offer relatively good protection from the primary fragments, but they can generate debris (window glass; i.e. Khobar towers bombing), concrete pieces, metal rods, pipes, part of the facade, sharp wooden debris). Also, some blast waves compromise objects structural integrity (collapse), crushing those who took shelter inside [3].

In previous period more than 4300 improvised explosive devices killed more than 65400 people (in 2014, over 75% of victims were non-combatants) [11].

When IED or high explosive munitions detonate in an urban area, blast waves (incident and reflected), together with fragments (primary and secondary), can cause large number of casualties. One notable example is 120 mm mortar attack in an enclosed public space (marketplace) in Sarajevo (1994), with the devastating effects (68 people killed and 144 wounded). That location was shelled again in 1995, and a number of traumatic brain injuries (trauma consistent with blast wave injuries) were reported. This marketplace is located

in the centre of the city, encircled by tall structures, which probably reflected and intensified the blast wave, increasing the severity of injuries caused by fragments [3].
A similar event of an urban environment attack occurred in Tuzla (1995), when 130 mm artillery projectile killed 71 and wounded 150. Primary fragments were the main cause of deaths but it is possible that blast wave reflection, intensification (causing also secondary fragments) and channelling resulted in a higher number of fatalities. When large aerial bombs are used in close quarter urban areas, people caught outside in the streets can sustain severe injuries [3].

2. External loading of structures

In the case of finite structures there are three types of interaction between the blast wave and objects. The first, called diffraction loading, is the interaction of a large-scale blast wave such as might be produced by a nuclear device or conventional charge with very high yield (illustrated in Figure 1a), where the blast wave engulfs the object. Here, movement of the object is minimized because of its size (diffraction target). The second category, called drag loading, involves large-scale blast wave acting on a smaller object (Fig. 1b). This type of target (called drag target) will also be engulfed but dynamic pressure translational force will move and further damage the target as well. Third is the case of a blast wave created by the explosion of a relatively small charge loading a larger structure (Figure 1c), where the response of individual components of the structure should to be separately analysed [9].

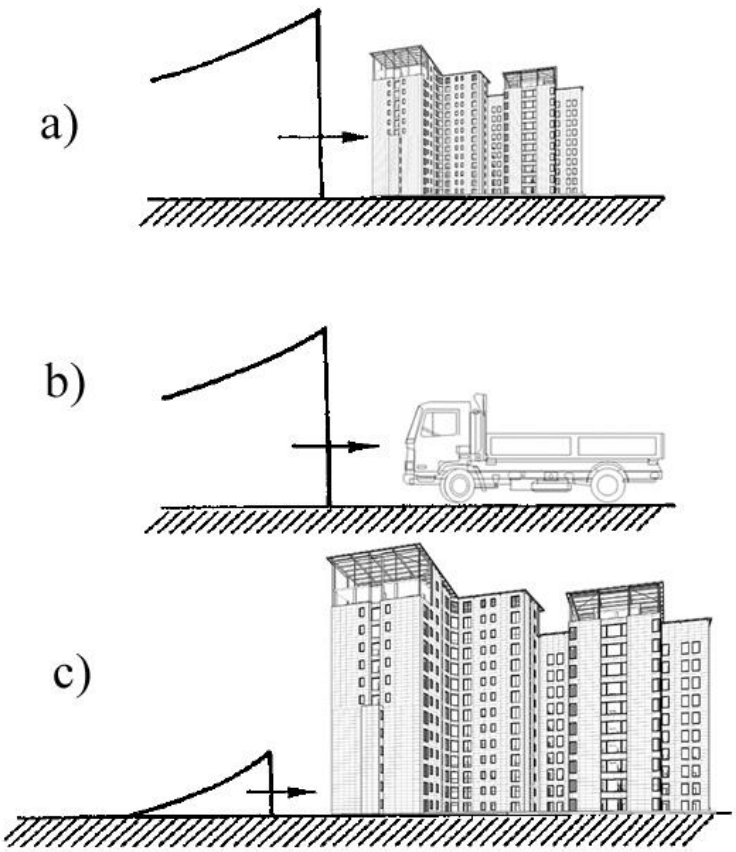

Figure 1. (a) Large explosion and relatively large object; (b) large scale explosion and rel. small object; (c) small scale explosion and rel. large object (adapted from [9])

The blast load on a structure depends on many parameters: explosion size, explosion location (confinement type), the geometry and orientation of the object, etc. [2]. The knowledge required to design blast resistant construction include dynamics, explosion physics, and physical security techniques. One of the military manuals which provide procedures for the designing protective structures is TM5-855-1 (restricted for use). This manual contains formulas for prediction of blast wave parameters, and can be used to estimate explosive loading on structures [7]. Manual UFC 3-340-02 [4] is another widely used publication for evaluation of structure resistance against the explosion blast.

Figure 2 shows schematically the main effects of a shock wave on objects, after the explosion. Figure 2(a) presents a structure (house), a nearby tree and small animal (in this case dog) before the wave arrives. Figure 2(b) shows objects after the passage of blast wave - large objects (house and tree) are encircled by wave (diffraction – blast wave loads all exposed surfaces). In this situation, the right wall of the house (towards the tree) is loaded by reflected and the front wall with incident overpressure. In that process, weaker structure elements (the glazing) will fail. But the house and the tree are firmly connected to the ground, and don't move under the blast load. Small animal experiences the same loading, but although being also engulfed by the blast waves (diffraction load), the dog responds more to the dynamic pressure (represented by moving air molecules behind the wave front). So, the dog is carried away along with the blast wind. Loosely fixed items on the house (the roof tiles, antennas) and the tree (leaves, smaller branches) are cut off by the dynamic pressure load. Figure 2(c) shows the same scene after the overpressure phase is finished. Figure 2(d) shows objects experiencing the underpressure phase (consequence of rarefaction and reversing air flow) [16].

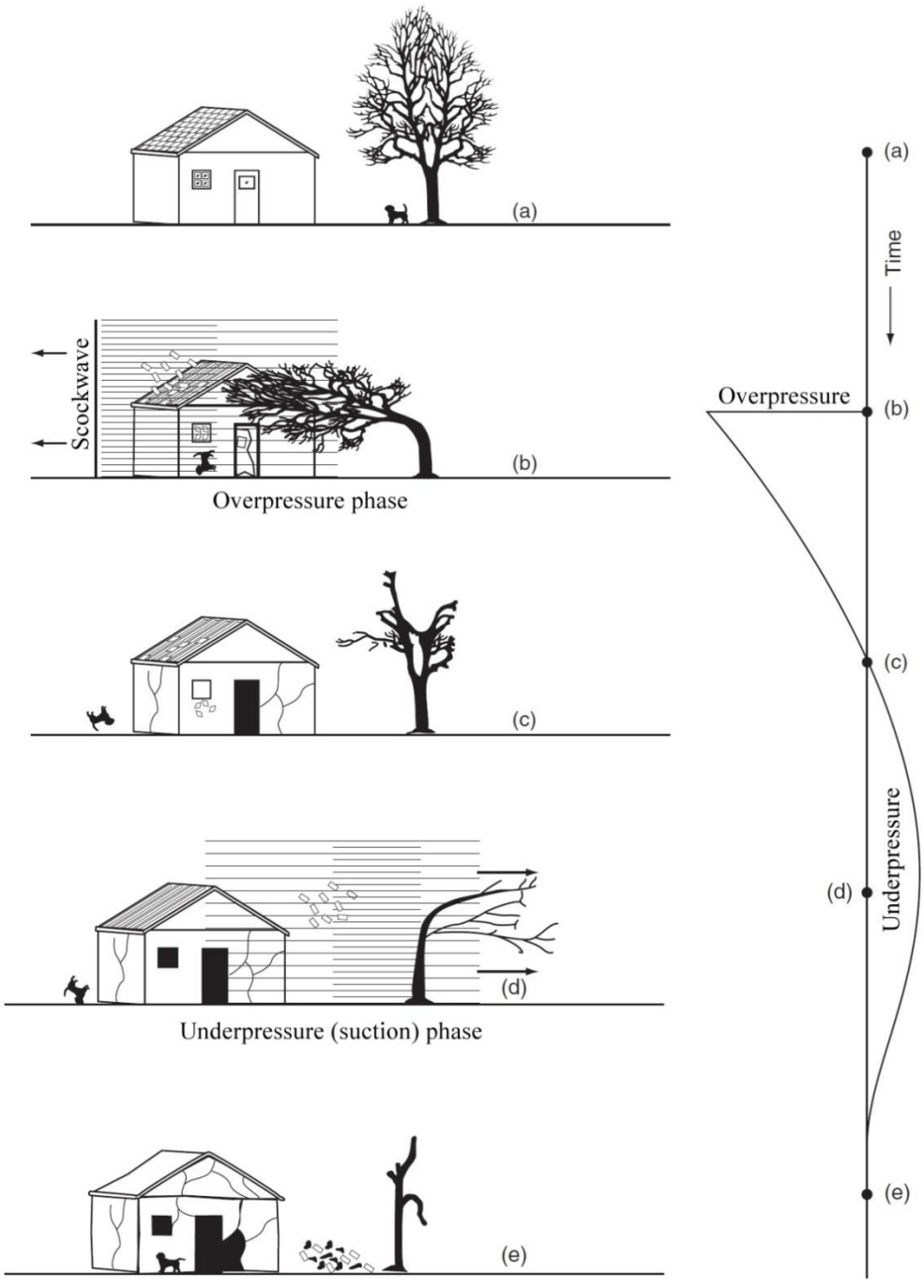

Figure 2. External blast load (adapted from [16])

2.1. Forces acting on structures/objects

The estimation methods for the external blast loads on objects, presented in this section (based on UFC 3-340-02 manual), are mostly used in the case of above-surface rectangular objects (other shapes and surface location can also be included in calculation) subjected to a plane shock wave front.
The forces acting on object loaded with a shock wave depend on the maximum overpressure and the impulse. Relationships are known between the peak dynamic pressure (q_o), the particle velocity, the peak incident pressure (P_{so}), and the density of air behind the shock wave. The particle velocity, dynamic pressures (important parameter for estimation of the loads on objects), and density of air depend on the peak incident pressure (as shown in Fig. 3) [4].

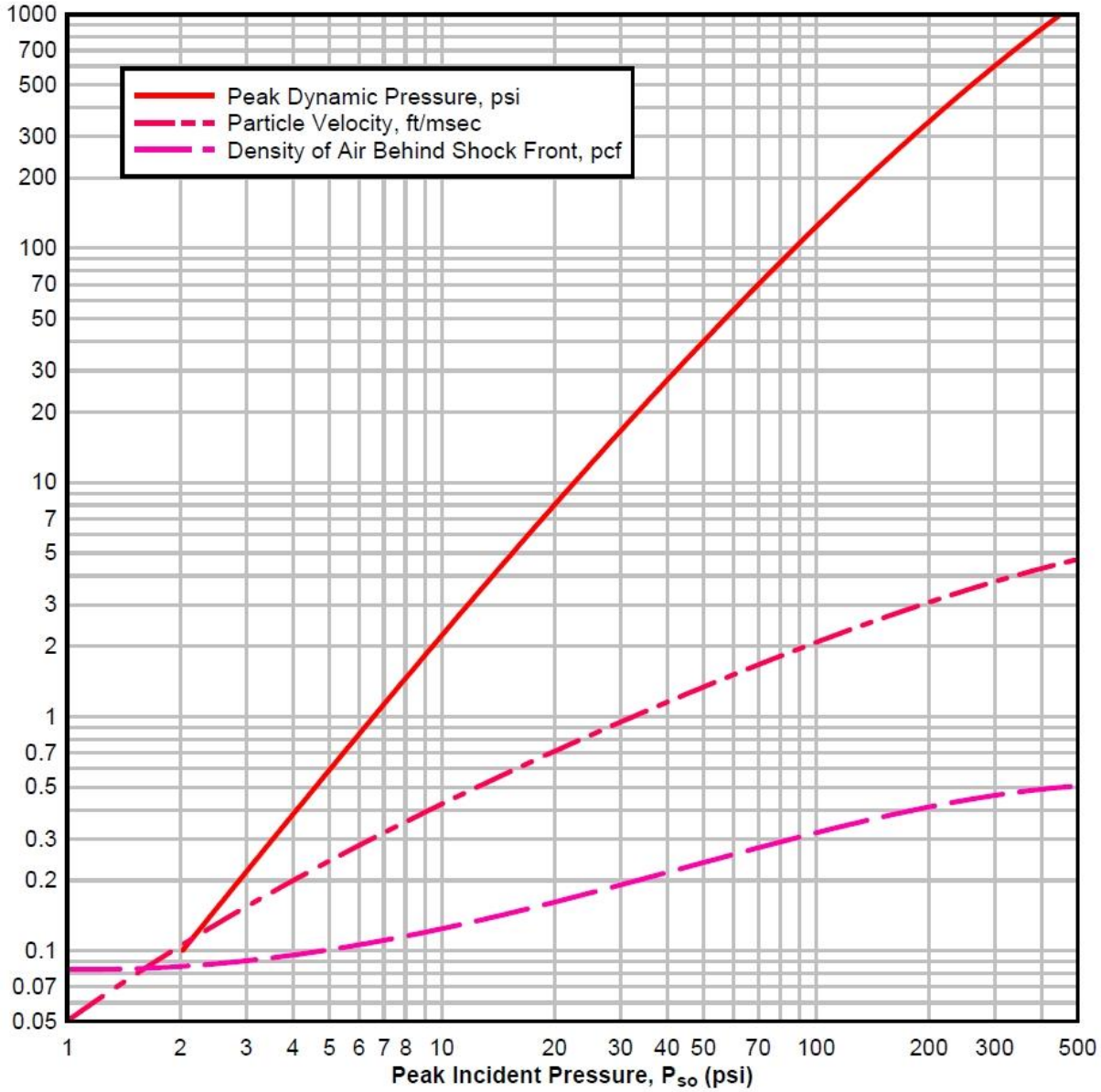

Figure 3. Relations between maximum incident pressures, maximum dynamic pressure, and density of air behind the shock wave front, and particle velocity (source: [4]);
(SI units: 1 psi = 6894,76 Pa, 1ft/msec = 304,8 m/s, 1 lb/ft^3 = 16 kg/m^3)

The effects on the objects subjected to an explosive blast load depend on the loading magnitude - time history and maximum intensity, so during the design process one needs to estimate the appropriate change of the dynamic and incident pressures during time.

Incident shock wave (Figure 4) is characterized by a rapid (almost discontinuous) increase in pressure to a certain maximum value, a period of decrease to an ambient pressure, followed by a period in which the pressure decreases below ambient.

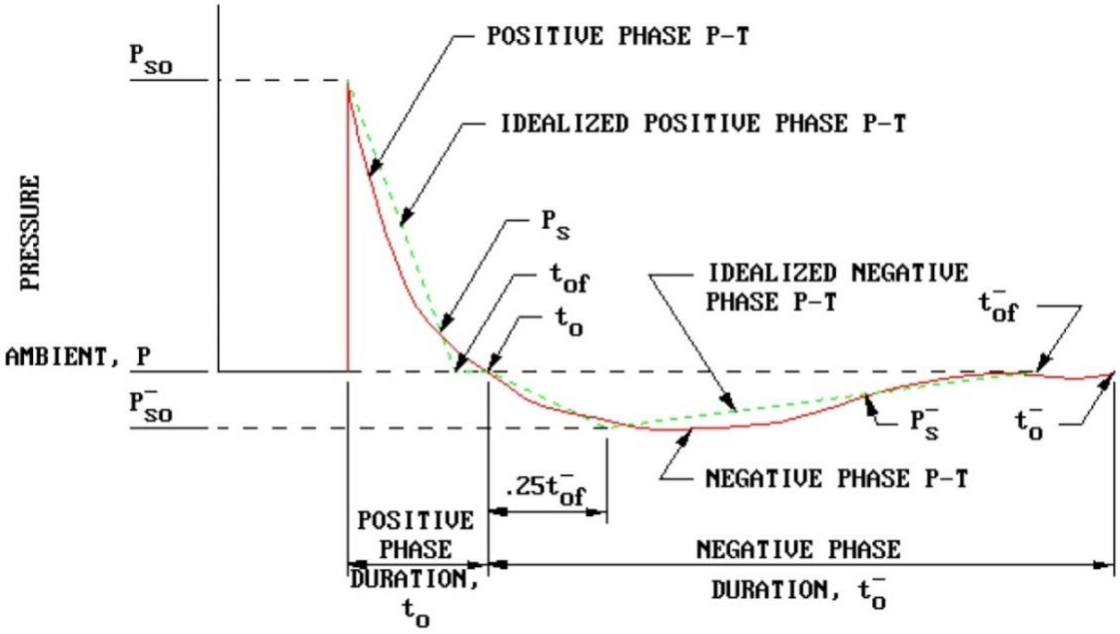

Figure 4. Idealized *P-t* variation (source: [4])

Variation of pressure with time is, generally, an exponential one, and some programs (i.e. CONWEP) take another approach, with exponential function of pressure decay with time (Friedlander equation) [7].
But the actual variation of the incident pressure can be successfully approximated by using so called "equivalent triangular pressure pulse" (Fig. 4) and estimated "manually", in a step-by-step manner. Here, the real positive phase duration is replaced by a "fictitious" one t_{of}, expressed with total impulse i of positive phase and maximum pressure P [4]:

$$t_{of} = \frac{2i}{P} \tag{1}$$

The formula (1) for the equivalent triangular pulse can be used for the incident and reflected pressures. For the negative phase, a similar method may be used, where the equivalent negative *P-t* curve will usually have a "rise" time of $0{,}25t_o$ and where t_{of^-} is given by [4]:

$$t_{of^-} = \frac{2i^-}{P^-} \tag{2}$$

Here i^- is total wave impulse and P^- maximum pressure of the negative pulse (of the incident or reflected waves). [4].

2.2. External loads on structures without openings

The forces acting on a structure can be classified as: the force from the dynamic pressure, the force from the incident pressure, the force from the reflection pressure, and the force from the negative phase pressure.
To reduce the difficulties involving the blast problems, certain simplifying assumptions can be made: the incident pressure is smaller than 13,7 bar, the object is rectangular, the loaded object is in the region of Mach stem, and the object height is lower than Mach stem [4].

2.2.1 Front Wall Loads

For above ground object, the pressure *P(t)* on the front face, for the case of normal reflection, is shown schematically in Fig. 5a.

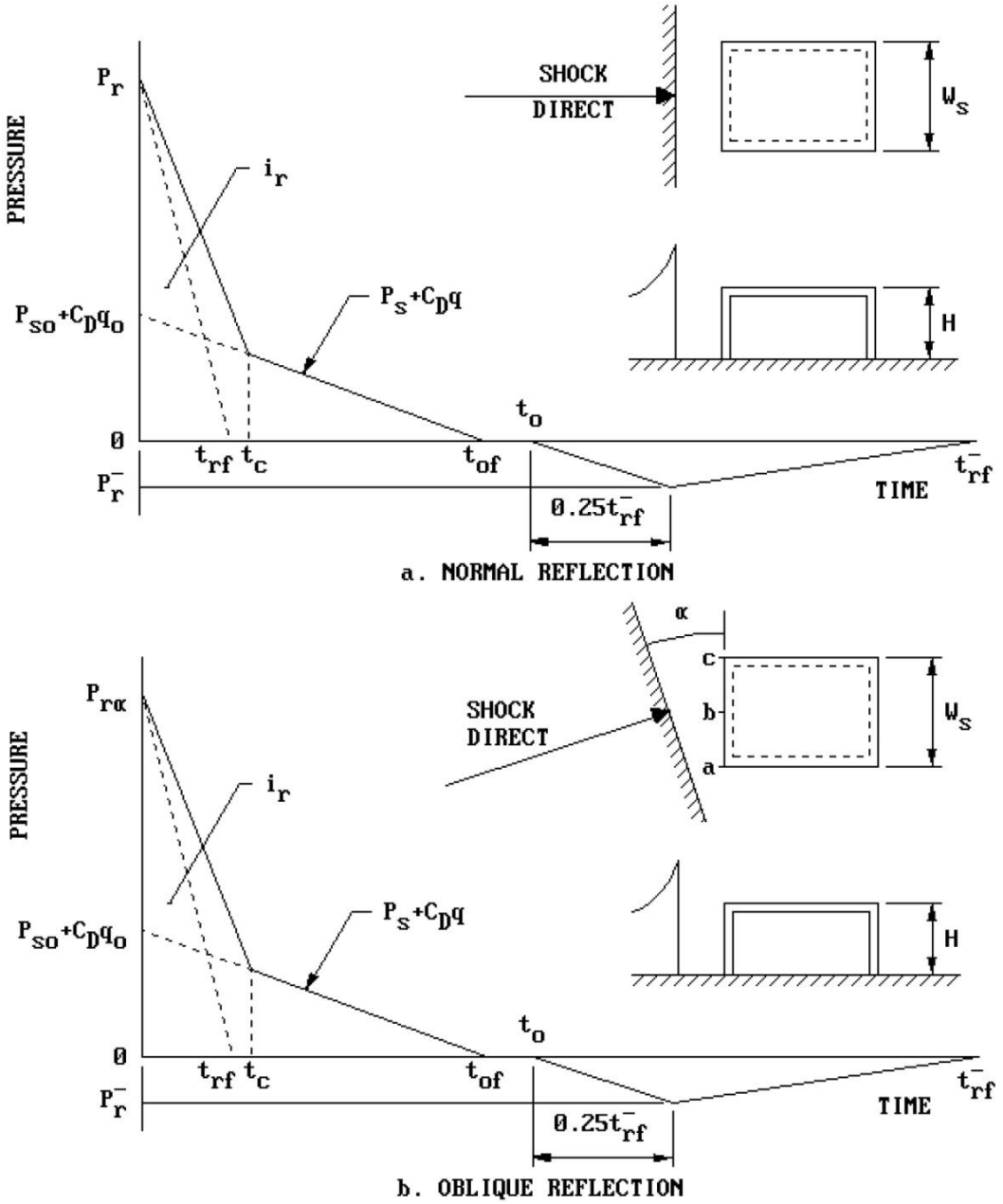

Figure 5. Front wall loading (source: [4])

When the incident shock wave impacts the front wall of the object, the pressure rises to normal reflected pressure P_r. The time for "relieving" the reflected pressure, also called clearing time t_c, is solved as [4,12]:

$$t_c = \frac{4S}{(1+R)C_r} \tag{3}$$

where S is "clearing" distance (H or $W/2$, whichever is the smallest; Fig. 5a), H – object height, R - S/G ratio (G is equal to H or $W/2$, whichever is larger; Fig. 5), and C_r is sound velocity in region of reflection (Fig. 7). The reflected pressure from the front of the object is relieved by the sides and roof leakage. Because of this, reflected pressure is reduced relatively quickly and becomes the sum of the side-on and the dynamic pressure. The time required for this is called clearing time t_c, mentioned in Eq (3) [8]. The clearing reduce the impulse to the front surface of an object compared with the impulse to an infinitely large object in which clearing would not be possible [16].

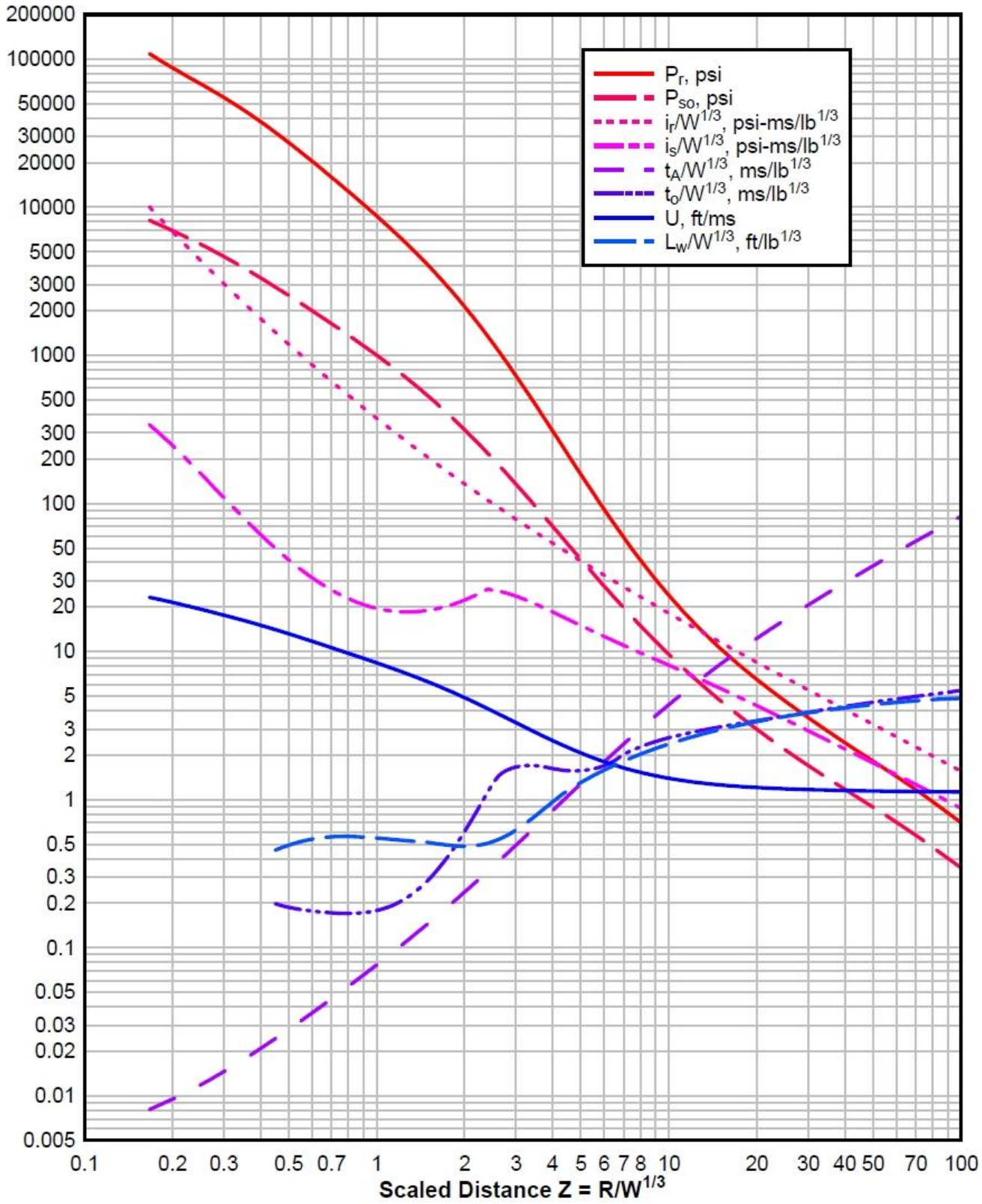

Figure 6. Different blast wave parameters for TNT explosion on the surface; imperial units (source: [4])

(SI units: 1 psi = 6894,76 Pa, 1 psi-ms/lb$^{1/3}$ = 8973,58 Pa-ms/kg$^{1/3}$, 1 ms/lb$^{1/3}$ = 1,3 ms/kg$^{1/3}$, 1 ft/ms = 0,3048 m/s, 1 ft/lb$^{1/3}$ = 0,3967 m/kg$^{1/3}$)

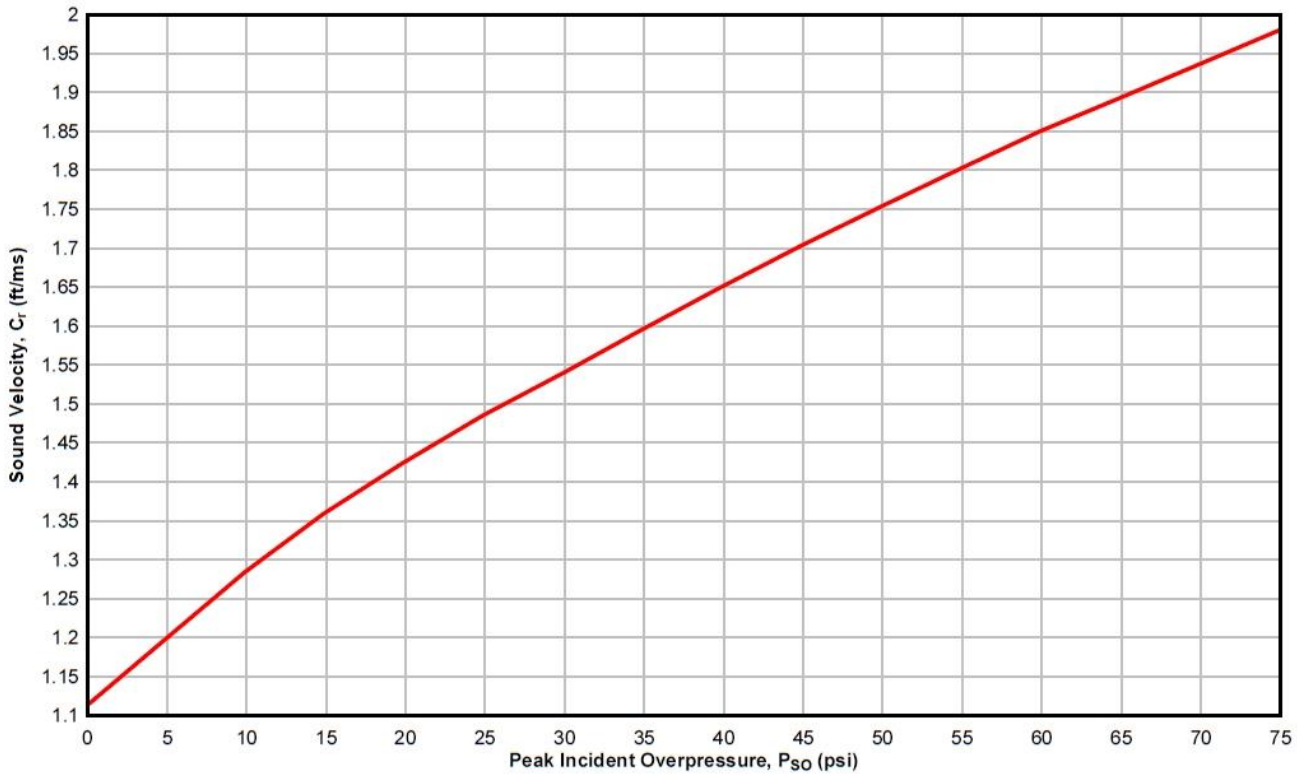

Figure 7. Sound velocity in reflected overpressure region as a function of maximum incident overpressure (source: [4]); (SI units: 1ft/ms = 304,8 m/s; 1 psi = 0,0689 bar)

The pressure on front wall after time t_c can be estimated by summation of the incident and the drag pressures [4,12,20]:

$$P = P_s + C_D q \tag{4}$$

The drag coefficient C_D depends on Mach number and object shape. For higher pressures, this method can give a "fictitious" *P-t* curve, so this must be checked by constructing another curve (triangle with dots in Fig. 5a) using the total impulse of reflected pressure i_r from Fig. 6 for a shock wave with a normal reflection (Fig. 5a). The "fictitious" duration t_{rf} for the wave with a normal reflection is determined using expression [4]:

$$t_{rf} = \frac{2i_r}{P_r} \tag{5}$$

where P_r is the maximum pressure with a normal reflection (Fig. 6). Curve (Fig. 5a) that shows the smallest value of the impulse is generally used in calculation of the wall loading. If the shock wave front hits the structure at a different angle (called oblique angle; Fig. 5b), the maximum pressure is a function of the incident pressure and the angle of incidence (diagram on Fig. 8). Following expression can be used for non-zero obliquity angle [4]:

$$t_{rf} = \frac{2i_{r\alpha}}{P_{r\alpha}} \tag{6}$$

Here peak reflected impulse $i_{r\alpha}$ is obtained from diagram on Fig. 10. Only the positive part of the *P-t* curve in Fig. 5b is used for the structure front wall construction.
The negative pressures should also be estimated in the process of the structure motion prediction. Here, the maximum reflected pressure in negative phase (Fig. 5) and reflected impulse can be obtained from Fig. 9 and correspond to the maximum incident pressure (Fig. 6) hitting the object front wall.

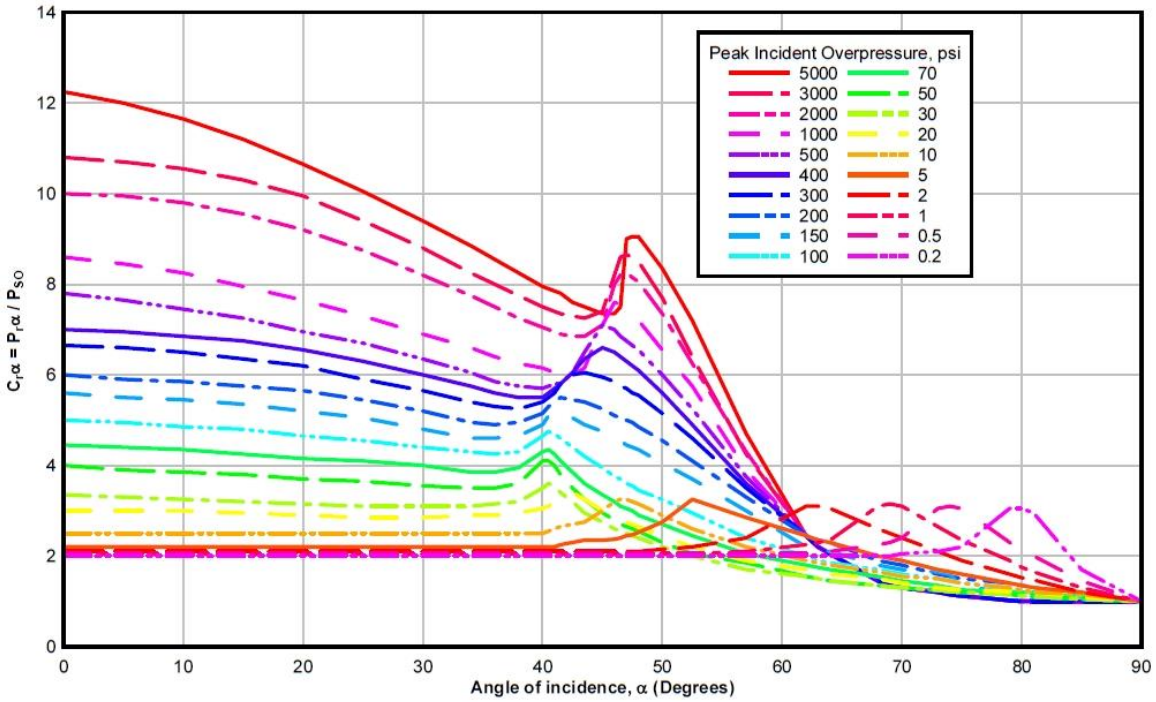

Figure 8. Reflected pressure coefficient versus angle of incidence (source: [4]);
(SI units: 1 psi = 6894,76 Pa = 0,0689 bar)

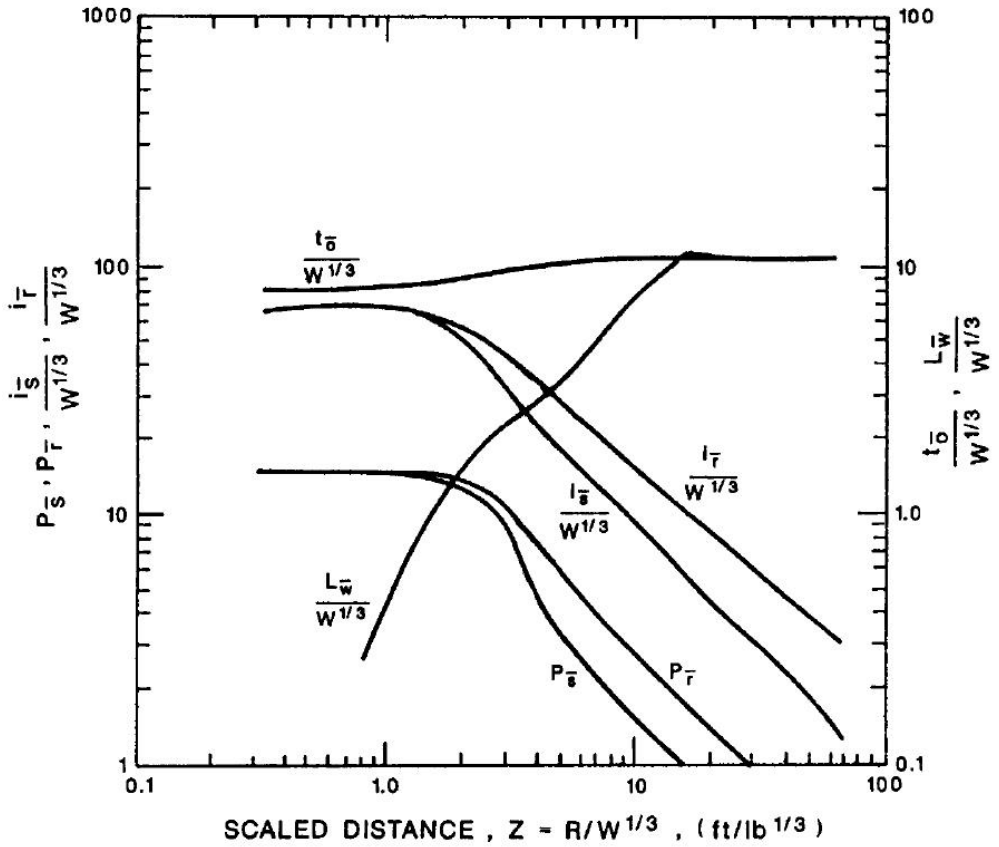

Figure 9. Blast wave parameters of negative phase for a TNT explosion on the surface (source: [4]);
(SI units: 1 psi = 6894,76 Pa, 1 psi-ms/lb$^{1/3}$ = 8973,58 Pa-ms/kg$^{1/3}$,
1 ms/lb$^{1/3}$ = 1,3 ms/kg$^{1/3}$, 1 ft/ms = 0,3048 m/s, 1 ft/lb$^{1/3}$ = 0,3967 m/kg$^{1/3}$)

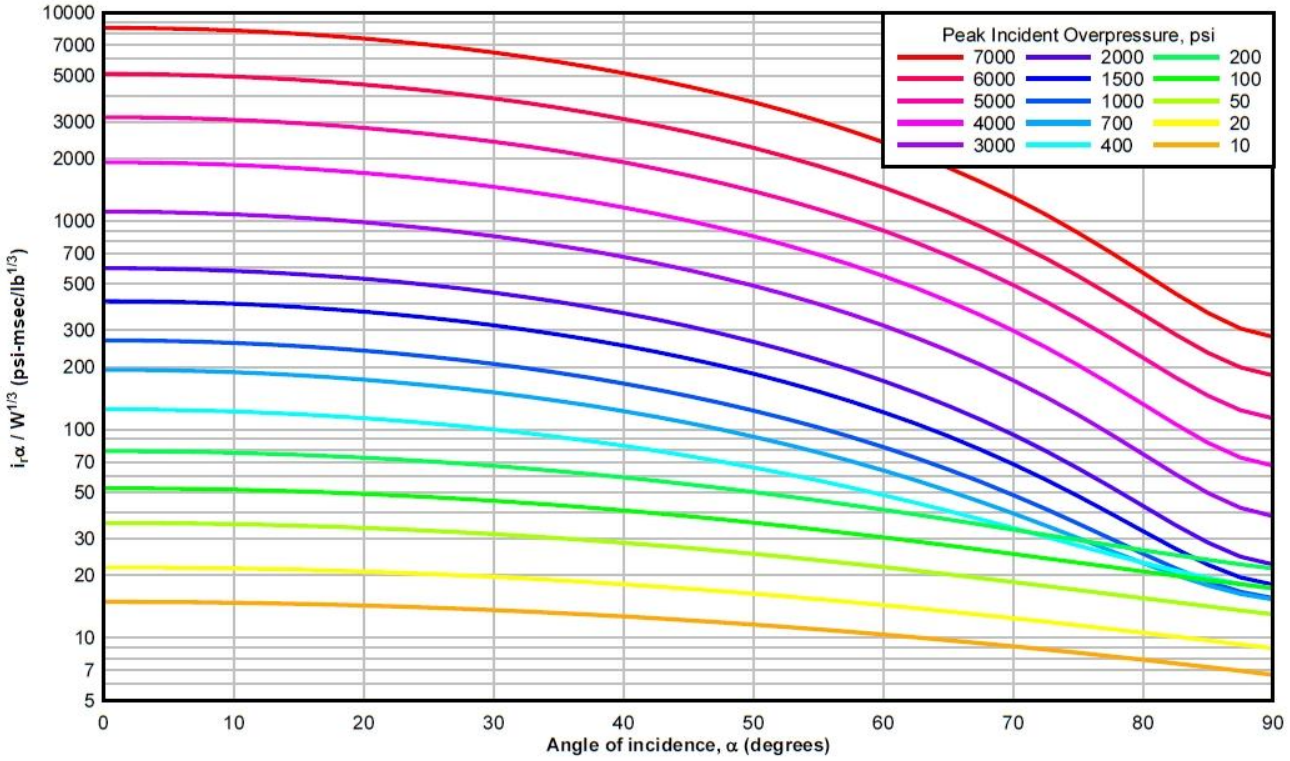

Figure 10a. Reflected scaled impulse versus angle of incidence for 10 - 7000 psi range (source: [4]);
(SI units: 1 psi-ms/$lb^{1/3}$ = 8973,58 Pa-ms/$kg^{1/3}$)

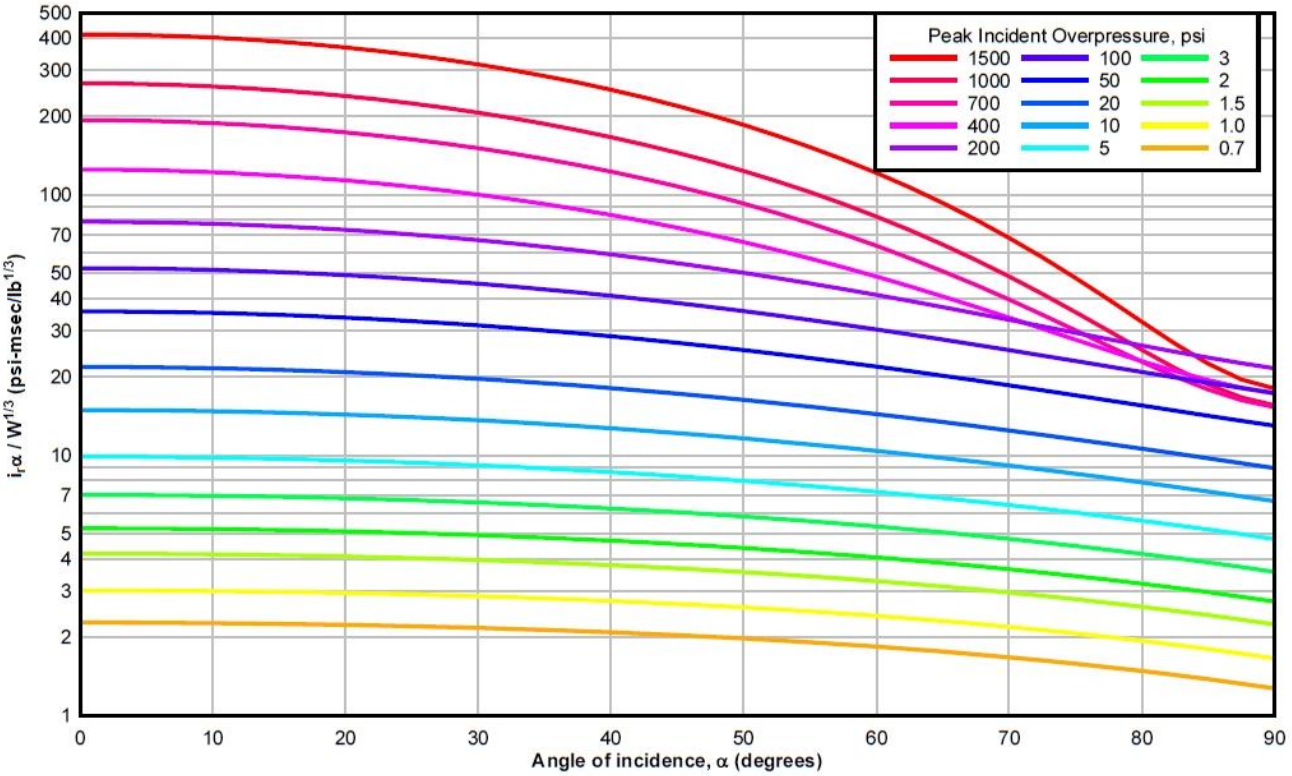

Figure 10b. Reflected scaled impulse versus angle of incidence for 0,7 - 1500 psi range (source: [4]);
(SI units: 1 psi-ms/$lb^{1/3}$ = 8973,58 Pa-ms/$kg^{1/3}$)

2.2.2 Roof and side walls

When blast wave traverses across the object, the upper (roof) and side walls are pressure loaded (incident pressure reduced by a negative drag pressure at a given time).
The part of the face loaded at a given time depends generally on the incident pressure, the location of the front wave and wavelength of positive (L_w) and negative phases (L_{w-}). To estimate total loading on a surface, one needs to analyse the wave movement across the face - this requires integration of the pressures at different locations (Figure 11a), to calculate the equivalent uniform incident pressure on a distance L (Fig. 11b).

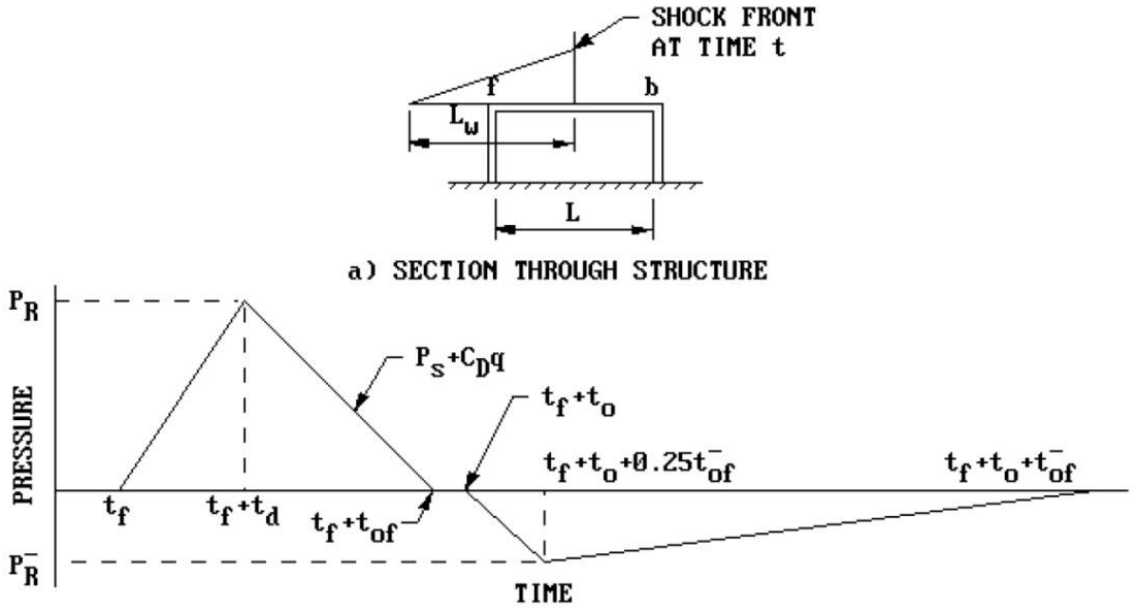

Figure 11. Roof and side wall loading (source: [4])

As shown in Fig. 11, the equivalent uniform pressure will rise in a linear fashion from t_f, when the shock wave approaches the front element of a structure (point f), to t_d, when the maximum equivalent uniform pressure is obtained. This pressure will after that decrease to zero at location b on the element.
The equivalent load factor C_E, the rise time, and duration of equivalent uniform pressure can be obtained from diagrams in Figures 12, 13, and 14, as a function of ratio L_{wf}/L.
The maximum pressure P_R acting on the roof can be estimated by summation of equivalent uniform and drag pressure [4]:

$$P_R = C_E P_{sof} + C_D q_{of} \tag{7}$$

Here P_{sof} represent the incident pressure (at point f), and q_{of} dynamic pressure (corresponding to $C_E P_{sof}$). Recommended values for C_D (for the upper and side walls depend on the maximum dynamic pressure) are presented in table 3.

Table 3. Recommended C_D values (Source: [4,13])

Loaded surface	Drag coefficient
Front	0,8 - 1,6
Rear	0,25 - 0,5
Side and roof (pressure dependent)	
0 - 172,4 kPa	-0.4
172,4 - 344,7 kPa	-0.3
344,7 - 896,3 kPa	-0.2

For overall motion of an object, the negative phase pressures effects should also be estimated during the procedure [4].

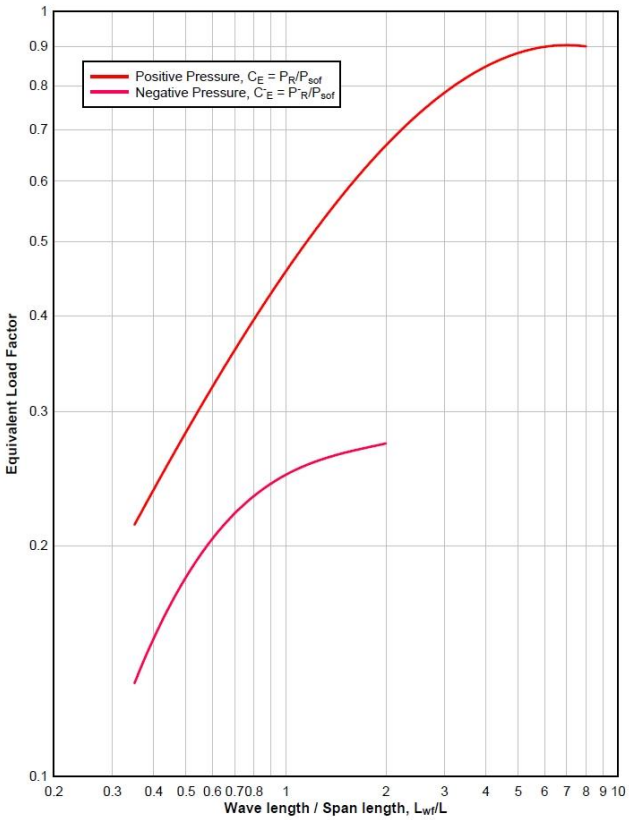

Figure 12. Maximum equivalent uniform upper surface (roof) pressures (source: [4])

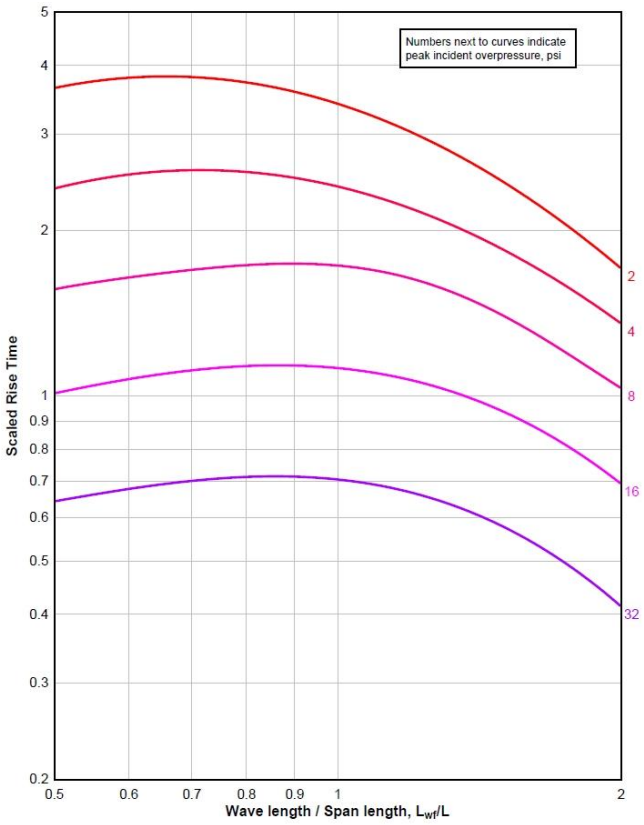

Figure 13. Scaled rise time of roof equivalent uniform positive pressures (source: [4]);

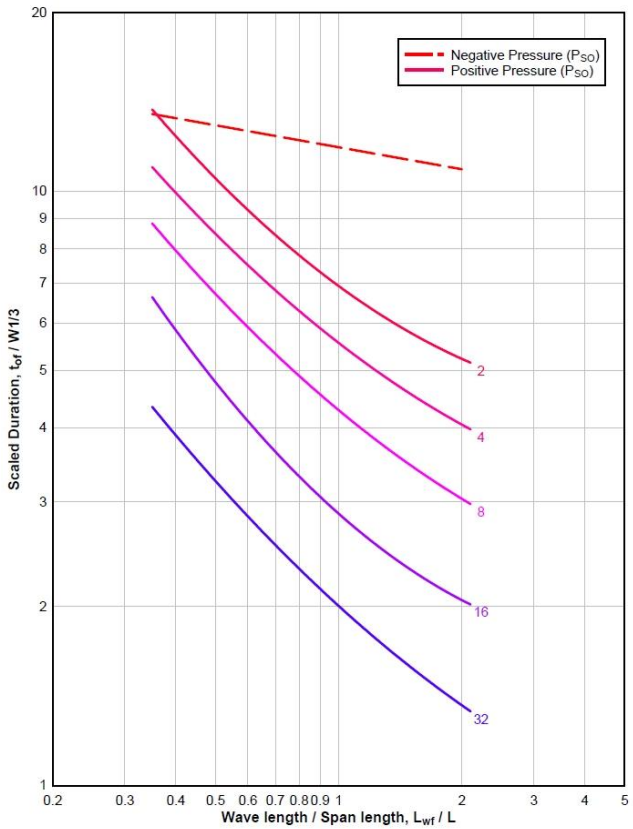

Figure 14. Scaled duration of roof equivalent uniform pressures (source: [4]);
(SI units: 1 psi = 6894,76 Pa = 0,0689 bar; 1 ms/lb$^{1/3}$ = 1,3 ms/kg$^{1/3}$)

2.2.3 Rear wall

The shockwave front will expand as the front crosses the rear/back parts of the roof and/or structural side walls, forming secondary waves moving over the back wall. The secondary wave engulfing the back wall results from the "spillover" from the roof, and the side walls, in the case of longer structures. These secondary waves are further strengthened after hitting reflecting surfaces.
In most construction cases, calculating the total drag effects on the building is the key justification for estimation of the blast loads on the rear wall.
The blast loading on the back wall (Fig. 15a) is estimated using the similar method as the one used for the blast loads on the upper surfaces (roof) and side walls of the object. Here the maximum pressure of the equivalent uniform *P-t* curve (Fig. 15b) is estimated using the maximum pressure P_{sob} that would develop at the back edge of the upper surface.
The equivalent uniform load factors (C_E, C_{E-}) are based on the maximum pressure values. The dynamic pressure corresponds to the one associated with the equivalent pressure $C_E P_{sob}$, and the drag coefficients recommendations are the similar as the ones used for the upper surface (roof) and side walls of given structure. [4].

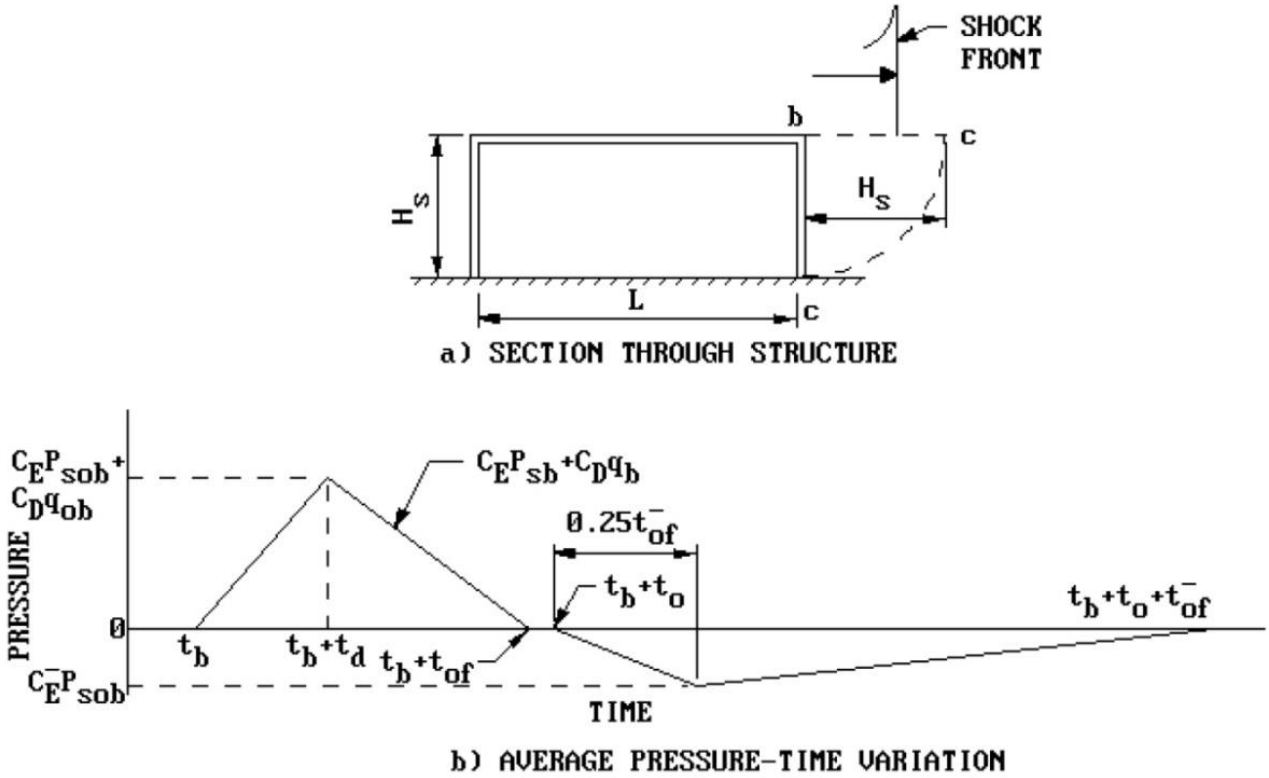

Figure 15. Rear wall loading (source: [4])

An examples of (manual) calculations of external load on structures and construction of approximate *P(t)* diagrams can be found in [4,8,10].

2.3. Influence of openings in the structure

To ensure sufficient light and ventilation, modern buildings contain wide gaps, typically on either side. Windows are the first components of the system that are expected to collapse when a blast wave reaches a structure. The prevailing theory of structural architecture allows them to be the weakest component of the structure, even though they are built to retain those pressure values, so failure of the wall before failure of the glass facade is naturally more risky.
When in contact with a standard window, the blast wave front automatically causes its collapse and it spreads inside the object. Around the same time, as some energy is consumed by the glass breakage [8], the maximum value of the overpressure wave will eventually become lower.

When blast loads are calculated on buildings with exposed openings on external faces, two structural configurations are commonly encountered. Windows, light doors or different openings situated in both the front and upper (roof) walls and along the structure's side walls are part of the first configuration. The second configuration encompasses openings found in the structure's front face only, and the other surfaces typically don't have openings.

When a shock wave front attacks a structure's front wall, the incident pressure is intensified. Windows and doors collapse almost instantly, unless they are designed to withstand the load. As a consequence, through these holes, blast wave fill the object. This abrupt release of high pressure will cause the inside of each opening to form a new shock wave front.

Each independent front will extend and appear to converge into a single wave front that expanding in the interior of the object. This internal shock is initially lower than the incident pressure of the wave on the outside of the structure but because of reflections, the interior pressure would eventually get larger.

In Fig. 16, an idealized structural object is presented. The arriving shock front has incident pressure P_{so} and wave length L_w. Blast wave penetrate the interior of the structure from the hole (opening) in the front part (with area A_0), as the shock front goes through the object. To achieve a hypothetical single opening centred at the middle of the front wall, the multiple openings area is usually determined (by summation of individual ones) [4].

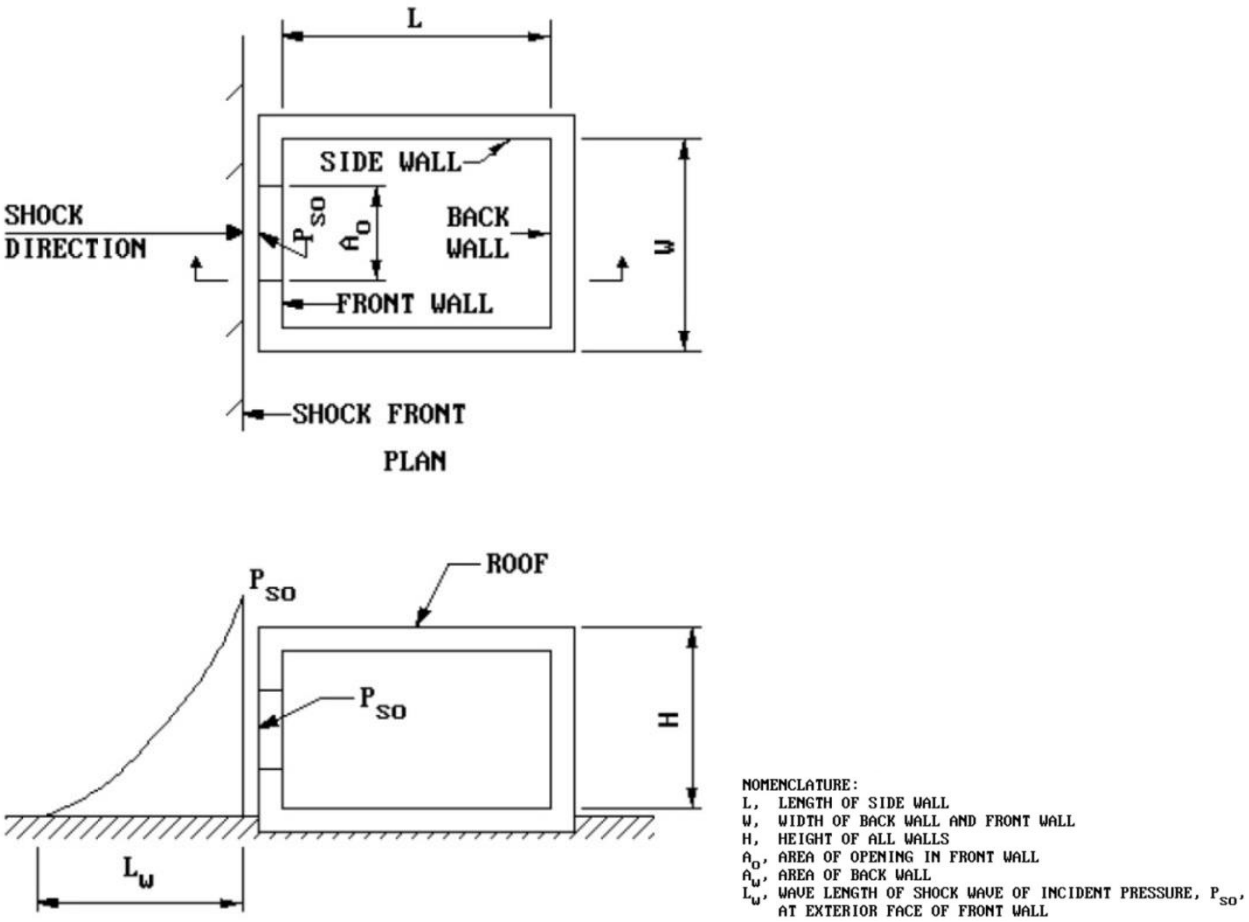

Figure 16. Idealized structure scheme for interior blast loads (source: [4])

Fig. 17 further illustrates the idealized *P-t* load curves for these (internal) surfaces inside a structure. The blast pressures operating on the outside of the building in residential area, except for the front wall, are not influenced by the opening in the object, and are calculated in compliance with the procedures mentioned in the preceding section.

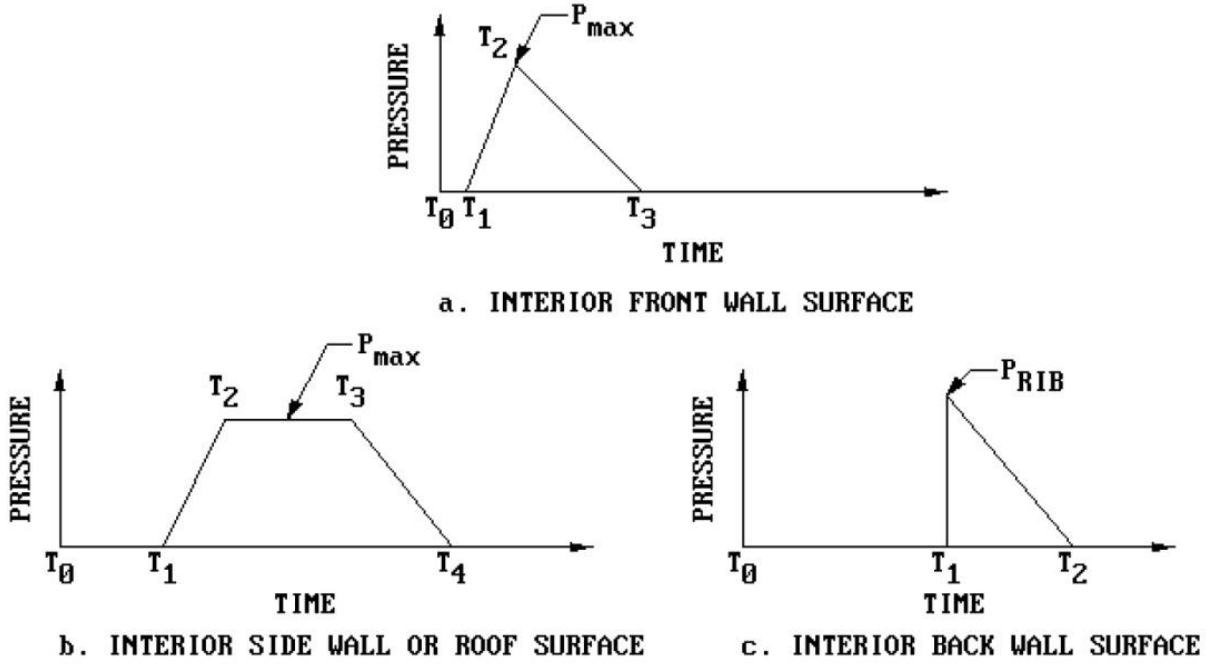

Figure 17. Idealized interior blast loads (source: [4])

As an example of software application for these cases, the CHAMBER code was developed to compute the pressure in a rectangular box-shaped room (structure) produced by the air blast from external explosions penetrating into the room through openings in the walls such as doors, windows and ducts of air entrainment systems [9].

3. Structural response to blast loading

When a shock wave hits an object, it generates a dynamic response, caused by the pressure and impulse transferred to the object [21].
The rate at which the impulse builds up is important since it can determine the strain rate of the target [22].
Blast load events induce large strain rates, approximately 10^2 - 10^4 s^{-1} [23]. The strength of structures is not only dependent on the load but also on structure characteristics, such as its geometry and materials. An object hit by a blast wave experiences a loading action which may cause deformation, and different damage levels can occur if the stresses and strains exceed those that the material can tolerate [9].
The deformation can take place in the entire structure when a blast wave hits the target, or can be built up in the central part, in the case of a localised blast wave, so the deflection response is dependent on the blast loading area. The magnitude and spatial distribution of blast loads on a given structure depends on several factors: characteristics of high-explosive materials, the stand-off distance, target or surroundings, and the amplification of the pressure pulse due to the reflection [24].
The natural period *T* of an object play an important role on its response [8]. Generally, three load regimes can be defined: impulsive, dynamic and quasi-static. The impulsive regime is present when the load pulse is short compared to the structure natural period of vibration: $\omega t_0 < 0{,}4$, where ω (= $2\pi/T$) is natural vibration frequency of an object. The dynamic regime occurs when the load duration and structural response times have similar order of magnitude: $0{,}4 < \omega t_0 < 40$. The quasi-static regime applies when the load duration is long compared to the structure natural response: $\omega t_0 > 40$. For impulsive loading, most of the deformation will occur after the blast load ended, and for quasi-static loading the blast will cause deformation of the structure while the loading is active [16].
The so called pressure - impulse (*P-I*) diagrams are used to define the limits for a safe response of structural member under different loading. Although these have been generally applied to predict structural damage, they can also be successfully used to predict human injuries due to the blast [16]. An example of a *P-I* diagram used frequently in blast analysis is shown in Figure 18, where the boundary contour line for a specific damage level is present [20].

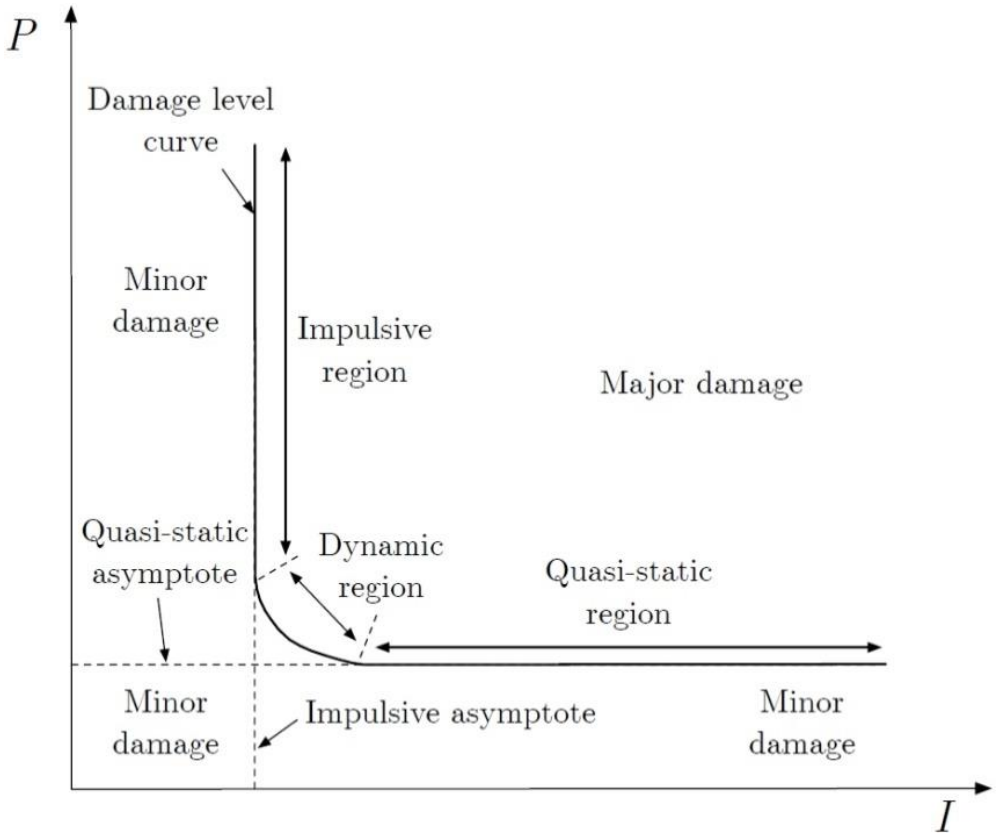

Figure 18. Typical pressure-impulse diagram (source: [20])

Diagram in Fig. 18 shows all the pressure - impulse combinations that generate the same damage level in a system. P-I diagrams are a representation of so called iso-damage curves [20].
There are two distinct regions in a pressure - impulse diagram (Fig. 18): significant structural damage and minor or no damage. P-I combinations to the left side and below given contour show responses below the corresponding damage level, and those above and to the right side of the contour will produce responses above the damage limit. For impulsive loads, the structural response is not dependent on the pressure.
The associated impulse is, however, the main parameter influencing the behaviour of the structure. For quasi-static loads the response depends on the pressure but on the impulse. The quasi-static asymptote is defined by the minimum pressure needed to reach a specific damage level. In between is a dynamic regime, which connects the impulsive asymptote with the quasi-static asymptote, and where the structural response depends on both pressure and impulse [20].
Designing structures to resist explosion blast waves is a very complex, and the evaluation of the structural strength under blast loads through computer simulations uses mainly two methods [20]:

- Computational Fluid Dynamics (CFD) which allows the study of interactions between a fluid and a solid structure (Fluid-Solid Interaction),
- Computational Solid Mechanics (CSM), dealing with response of the structure.

4. Numerical simulations

The empirical method outlined in the previous section permits estimation of explosive shock wave effects mostly for isolated structures. Structure complex geometry, other structures in proximity, and the surrounding environment cannot be taken into account using exclusively these methods. Also, the simplified empirical techniques give relatively good agreement with the test data only for the structure sides situated on the front surface. To overcome these limitations, various CFD (eng. Computational Fluid Dynamics) methods and Hydrocodes (large computer programs used to numerically simulate dynamic events, particularly those which include shocks) are used for prediction of blast load on the objects. [18].
Numerical simulations in this paper were performed in Ansys AUTODYN program.

When simulating explosions, material properties can be selected from the AUTODYN material library. Air uses the equation of state for Ideal gas, where the pressure P is related to the energy e (with adiabatic exponent γ) [25] as:

$$P = (\gamma - 1)\rho e \tag{8}$$

This form of an equation is useful for its simplicity and computation ease, where only the value of γ needs to be supplied.
For high explosives (ie TNT), there are different forms of equations of state (Ideal gas, Constant Beta, Wilkins, Becker-Kistiakowski-Wilson), but the one used in AUTODYN is Jones - Wilkins - Lee (JWL), in the following form [25]:

$$p = A\left[1 - \left(\frac{\omega}{R_1 v}\right)\right] \cdot e^{-r_1 v} + B\left[1 - \left(\frac{\omega}{R_2 v}\right)\right] \cdot e^{-r_2 v} + \frac{\omega e}{v} \tag{9}$$

The values of A, R_1, B, R_2, and ω constants from Eq. (9) have been determined from dynamic experiments (i.e. cylinder test) for many explosive types, and are available in AUTODYN material library.
In this research, as a validation of the AUTODYN program method for solving urban blast problems, we numerically simulated blast wave formation in a 3D urban scene (Fig. 19) and compared obtained results to the ones experimentally studied in reference [15].
Seven buildings of different heights (Fig. 19) simulated the cityscape. The experiment [1] used scaled urban scenarios where buildings B1, B2, and B4 were 400 mm high, buildings B3 and B5 300 mm high, and buildings RW and LW 450 mm high. The TNT charge with a mass of 16 g (charge radius of 13,28 mm), and a density of 1630 kg/m^3, was detonated at the point located 40mm above the ground between buildings. In relation to the origin coordinate system, the detonation point was located at following coordinates: 478 mm, 350 mm, 40 mm. Pressure measuring (gauge) point was located at following coordinates: 302 mm, 1100 mm, 105 mm.

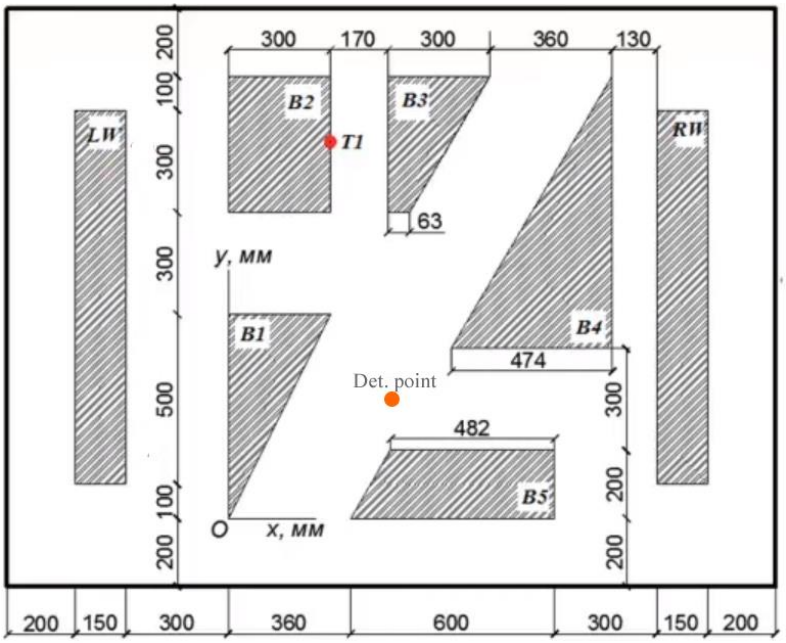

Figure 19. Initial setup of an urban environment explosion scenario (adapted from [1])

To numerically simulate the experiment [1] with an urban blast, a 3D numerical simulation was required. As a first step we used CAD (Computer-Aided Design) software to make a 3D model of the buildings, export the model as .iges universal document type, and imported it into Ansys Workbench (this can also be done in Ansys Geometry Modeler). In this way, one can import any urban area CAD model available.

The next step was to do a 2D axisymmetric numerical simulation of free airblast in AUTODYN, with given explosive charge geometry (13,28 mm radius). Mesh cells were 1 mm in size.
Values for different materials equations of state, as well as other material parameters, were specified from the default AUTODYN material library. Zones with air were defined with energy of $2{,}068 \cdot 10^5$ mJ/mm^3 (to obtain an environmental pressure of 101,3 kPa) - initial condition. Results of this simulation were saved and later remapped into an urban environment (remap origin coordinates were chosen as in experiment [1], Fig. 19) in 3D AUTODYN. Next we specified coordinate system origin and initial conditions in Ansys Workbench (earth gravity, and fixed, rigid buildings), and exported files into AUTODYN where the following procedure was used:

- Loading of air and TNT as materials (with default parameter values from AUTODYN material library).
- Specifying the initial condition (air was given initial energy of $2{,}068 \cdot 10^5$ mJ/mm^3).
- The flowout boundary condition was specified to eliminate the wave reflection at the end of spatial domain.
- Rectangular space grid was specified around buildings, and filled with air. Two Euler solvers were used (separately): Euler - Godunov and Euler - FCT, for the comparation of the results.
- With Euler - Godunov solver we conducted simulations with two mesh cell sizes, 20 mm (336175 cells) and 10 mm (2768500 cells), to conduct a mesh independence study. With Euler - FCT solver we conducted all simulations with cell size of 10 mm (total 2768500 cells), but with two different quadratic viscosities (1 and 0,1), since reference [26] suggest values of 0,1 as more accurate.
- Remapping of earlier 2D simulation results into 3D AUTODYN urban environment (coordinate point for detonation was specified as in the experiment, Fig. 19).
- Specifying gauge point location as in the experiment.
- Specifying simulation end time of 5 s (enough time for a pressure wave to engulf the structures).
- Specifying parallel processing method. Simulation run time (for 5s of simulation) with 2768500 cells was around 7h using octa-core processor (AMD Ryzen 7).

Fig. 20 shows pressure profiles determined with Euler solvers, compared (validated) to test data [1]. All solvers predict the event adequately, but FCT solver generally agrees better with test data, a conclusion also confirmed in [18]. Regarding mesh independence, there were no large qualitative differences in results between curves obtained with 10 mm and 20 mm cell sizes (see Euler - Godunov curves in Fig. 20), but smaller mesh size grid does give better prediction of the peak pressure. Regarding quadratic viscosities, values of 0,1 agree somewhat better with test data than the values of 1, a conclusion confirmed also in [26].

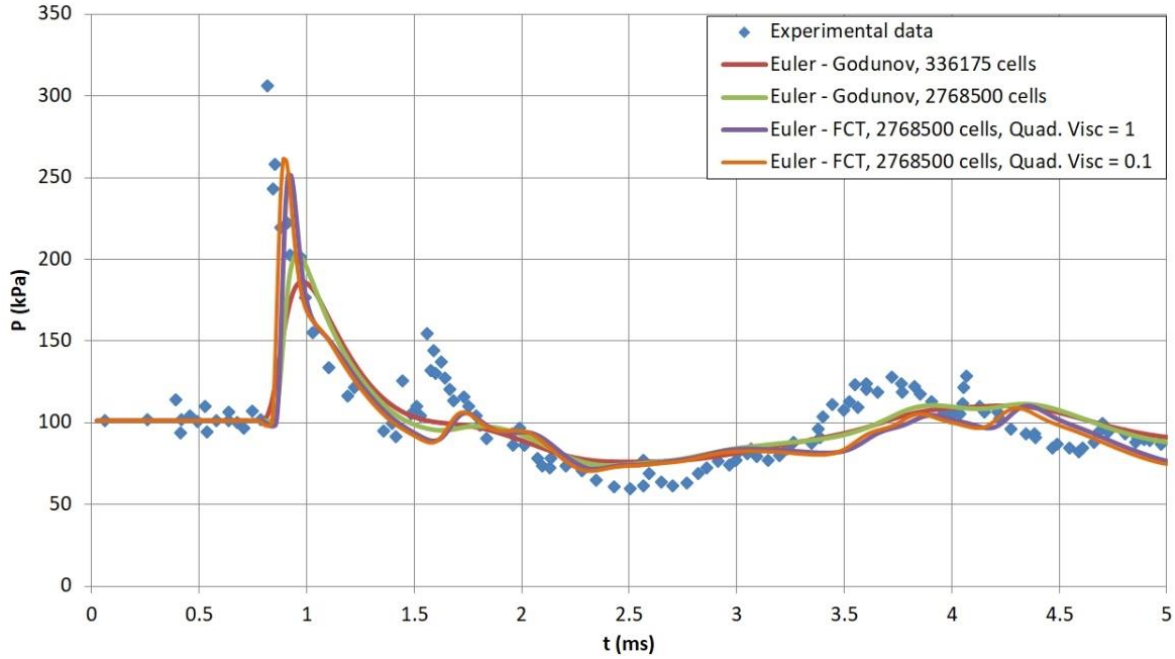

Figure 20. Pressures profiles determined with Euler solvers, compared to experimental data [1]

Fig. 21 presents pressure contours for different simulation times, showing wave reflections, diffraction around corners, and wave channeling due to the urban environment structures.
For the pressure contours section plane (Fig. 21) we selected height of 13,6 mm above ground (average human height level) since, for the mentioned scaled experiment [1], buildings had an average height of 400 mm. Namely, if we assume these buildings were in reality around 50 m high, then the value of 13,6 mm (for a horizontal section plane) in a simulation would correspond roughly to an average human height of 1,75 m in real case scenario.

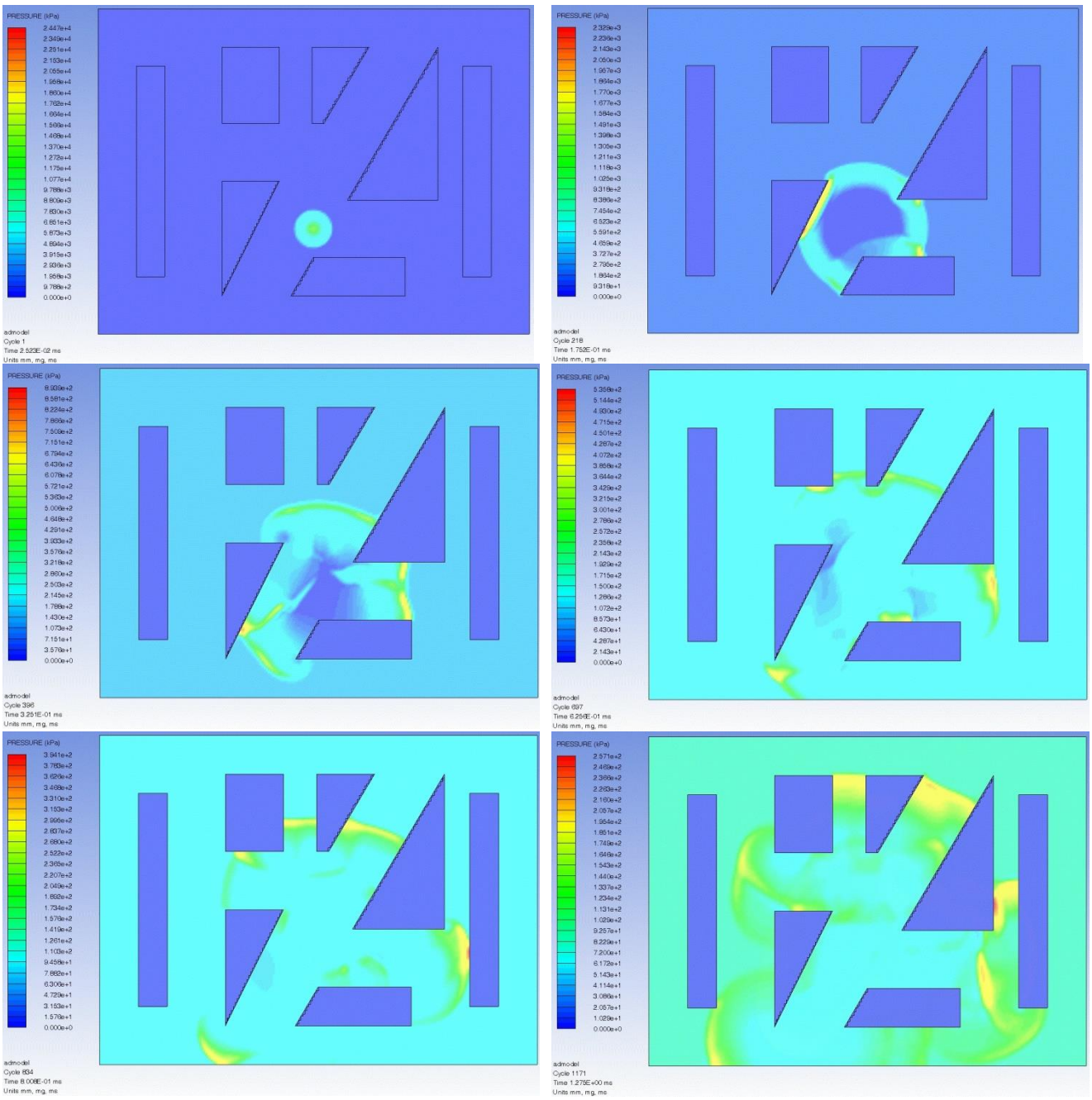

Figure 21. Pressure contours for different simulation times

Fig. 22 presents shockwave velocity vectors for different numerical simulation times. Here, the view is isometric and shows adequately the 3D model of buildings in AUTODYN. In Fig. 22 we can see the movement of the shockwave and its velocity at different times. Also, wave reflections and superposition can be seen as a wave develops further away from the detonation point. The last sequence in Fig. 22 shows that shockwave reaches the furthest buildings in this (scaled) urban model in about 2,25 ms.

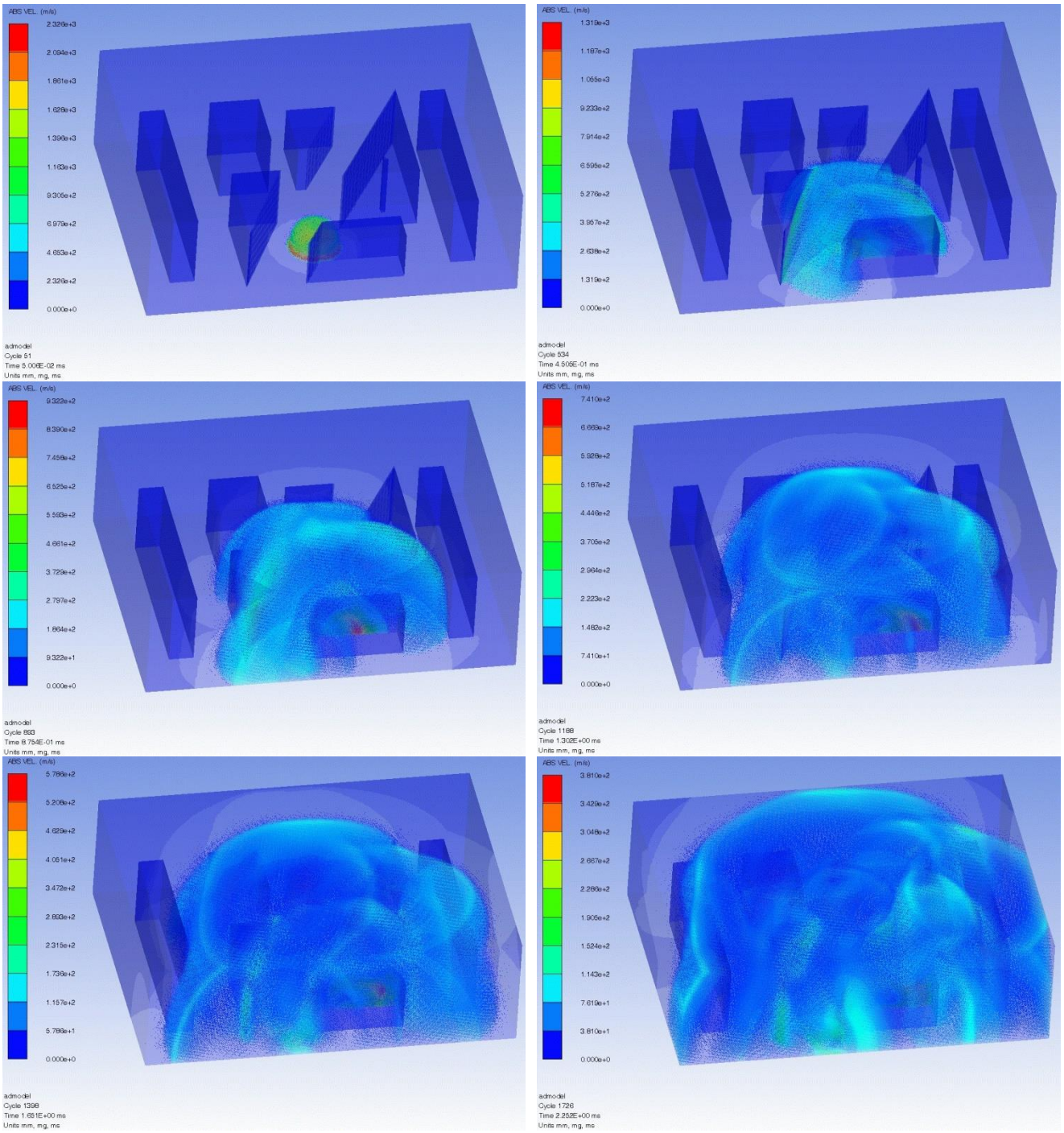

Figure 22. Velocity vectors for different simulation times

Fig. 23 shows temperature profile, determined with Euler - FCT solver, for test gauge (measuring point) T1 (shown schematically in Fig. 19). We see that the profile is similar as in the case for pressure, with maximum values for temperature of around 393 K (120 °C).

Fig. 24 presents temperature contours for different simulation times. Note that the scales in contours, presented in Fig. 24, are not the same in different time sequence.

Here, as in the Fig. 21, temperature contours section plane had height of 13,6 mm above ground, which correspond to an average human height of 1,75 m in real case scenario.

As can be seen from Fig. 24, the temperature quickly decreases as time progresses, and the closest buildings are impacted the most.

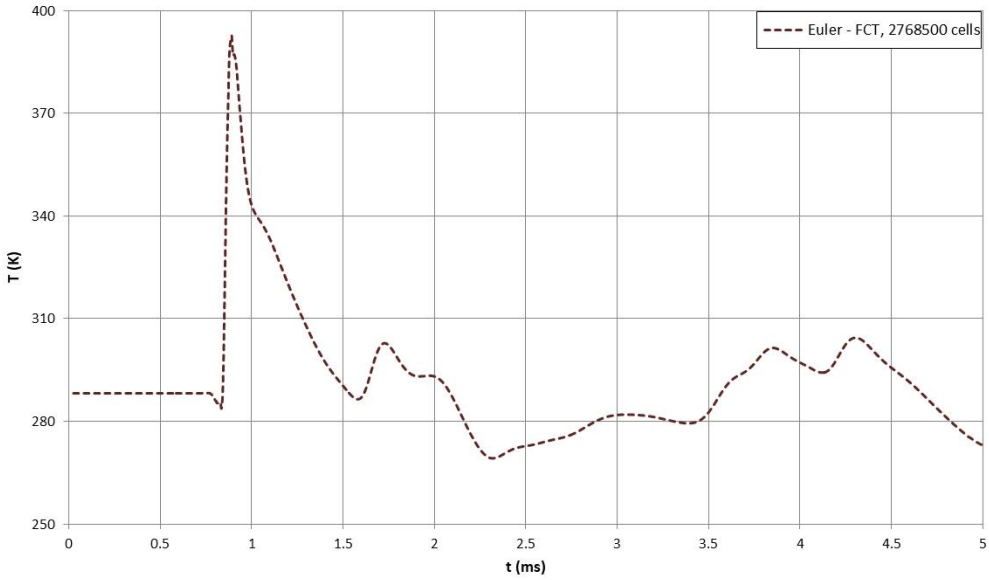

Figure 23. Temperature profiles at gauge point T1 (gauge is shown in Fig. 19)

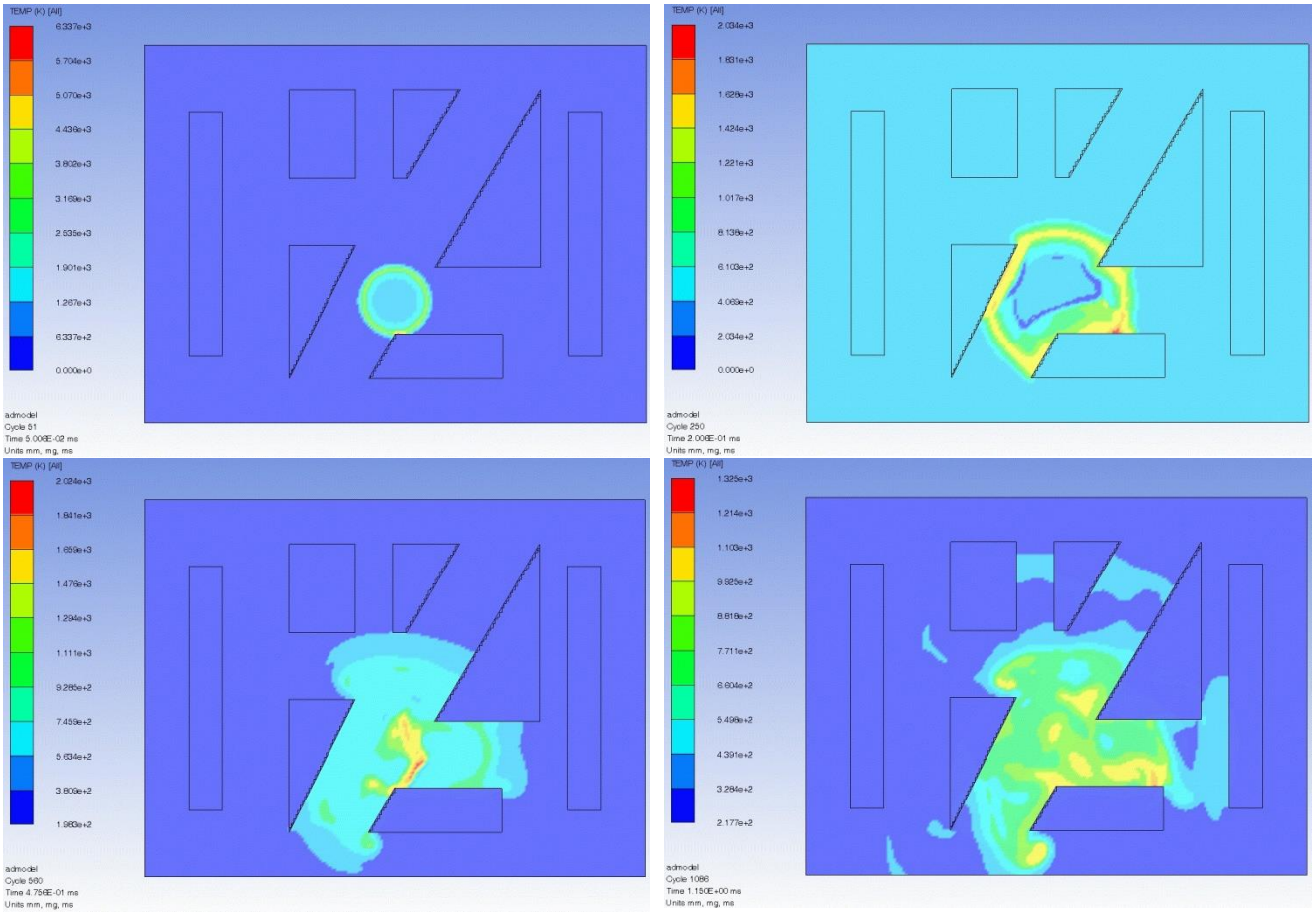

Figure 24. Temperature contours for different simulation times

Analysis of blast wave effects for complex geometry urban scenario is becoming an increasingly relevant topic since the number of terrorist attacks, and also accidents with explosive material are not decreasing.
Further research could be directed towards interior blast scenario. Also, work could be directed to using GIS files in a populated environment blast simulation, as a method for estimation of explosion effect in a real case scenario for certain urban areas. Methods for reinforcing the structures to the blast load could also be pursued in future research.

5. Conclusion

A review of external blast loads on structures modeling methods is presented in the paper. Numerical simulations of explosion in an urban scenario were done in software Ansys AUTODYN, and results compared to experimental values. Recommendations were given regarding the use of numerical simulations in blast wave parameter calculations for the urban environment.
Further research could be directed towards interior blast scenario. Also, work could be directed to using GIS files in a populated environment blast simulation, as a method for estimation of explosion effect in a real case scenario for certain urban areas. Methods for reinforcing the structures to the blast load could also be pursued in future research.

References

[1] M. A. Brittle, Blast propagation in a geometrically complex environment, Thesis, Craneld University, Defence College of Management and Technology, Shrivenham, Swindon, SN6 8LA, UK, July 2004.
[2] Military explosives, US Army Technical Manual, TM 9-1300-214, Sept. 1984.
[3] "Explosive weapon effects", GICHD, Geneva, ISBN: 978-2-940369-61-4, February 2017.
[4] UFC 3-340-02, Structures To Resist The Effects Of Accidental Explosions, Technical manual, Dec. 2008.
[5] Engineering Design handbook. Explosions in Air. Part One, Army Materiel Command, Alexandria, Virginia, 15 July 1974.
[6] M. L. Costa Neto, G. N. Doz, "Study of blast wave overpressures using the computational fluid dynamics", Rev. IBRACON Estrut. Mater. vol.10 no.3 São Paulo, May/June 2017.
[7] A. M. Remenikov, "The state of the art of explosive loads characterisation", Journal Of Battlefield Technology, Vol 6, No 3, 2003.
[8] V. Karlos, G. Solomos, "Calculation of Blast Loads for Application to Structural Components", Joint Research Center, 2013.
[9] P. D. Smith, J. G. Hetherington, Blast and Ballistic Loading of Structures, Butterworth-Heinemann Ltd 1994.
[10] A. M. Remenikov, "Blast Resistant Consulting: A New Challenge for Structural Engineers", Australian Journal of Structural Engineering · January 2002.
[11] "Improvised Explosive Devices (IEDs) - Publication", UN, Office for Dissarmament Affairs, https://www.un.org/disarmament/convarms/ieds2/.
[12] P. S. Bulson, Explosive Loading of Engineering Structures, Chapman and Hall, 1997.
[13] H. Draganic, V. Sigmund, "Blast loading on structures", Tehnički vjesnik 19, 3(2012), 643-652.
[14] S. E. Rigby, T. J. Lodge, S. Alotaibi, A. D. Barr, S. D. Clarke, G. S. Langdon, A. Tyas, "Preliminary yield estimation of the 2020 Beirut explosion using video footage from social media". Shock Waves. doi:10.1007/s00193-020-00970-z. ISSN 1432-2153.
[15] AUTODYN®, Material library, Ansys Inc, 2019.
[16] D. Cormie, G. Mays, P. Smith, Blast effects on buildings, Second edition, Thomas Telford Publications, 2009.
[17] N. Birnbaum, R. Clegg, G. Fairlie, C. Hayhurst, N. Francis, "Analysis of blast loads on buildings", Structures under Extreme Loading Conditions, 1996.
[18] N. N. Fedorova, S. A. Valger, A. V. Fedorov, "Simulation of blast action on civil structures using Ansys AUTODYN", International Conference on the Methods of Aerophysical Research (ICMAR 2016), AIP Conf. Proc. 1770, 020016-1–020016-10; doi: 10.1063/1.4963939.
[19] W. E. Baker, P. A. Cox, P. S. Westine, J. J. Kulesz, R. A. Strehlow, Explosion Hazards and Evaluation. Elsevier, 1983.
[20] A. Cacoilo, "Blast wave propagation in confined spaces and its action on structures", PhD Thesis, The University of Edinburgh, 2019.
[21] C. E. Needham, Blast waves, Second Edition, Springer, 2018.
[22] A. Wright, M. French, "The response of carbon fibre composites to blast loading via the Europa CAFV programme", Journal of Materials Science, 43(20):6619–6629, 2008. ISSN 0022-2461, 1573-4803. doi: 10.1007/s10853-008-2787-7.
[23] T. Ngo, P. Mendis, A. Gupta, J. Ramsay, "Blast loading and blast effects on structures - an overview", Electronic Journal of Structural Engineering, 2007.
[24] F.E.M.A. Reference manual to mitigate potential terrorist attacks against buildings. Technical Report FEMA 426, Department of Homeland Security, US, 2003.
[25] AUTODYN®, Explicit Software for Nonlinear Dynamics, Theory Manual Revision 4.3, 2005.
[26] T. C. Chapman, T. A Rose, P. D. Smith, "Blast wave simulation using AUTODYN2D: A parametric study", Int. J. Impact Engng, Vol 16, No 5/6, pp. 777-787, 1995.